

# Minimum in Diffusion Coefficient with Increasing MWCNT Concentration Requires Tracer Molecules To Be Larger than Nanotubes

Minfang Mu,<sup>†</sup> Russell J. Composto,<sup>†</sup> Nigel Clarke,<sup>‡</sup> and Karen I. Winey<sup>\*†</sup>

<sup>†</sup>Department of Materials Science and Engineering, University of Pennsylvania, Philadelphia, Pennsylvania 19104-6272, and <sup>‡</sup>Department of Chemistry, Durham University, Durham DH1 3LE, United Kingdom

Received June 30, 2009; Revised Manuscript Received October 2, 2009

**ABSTRACT:** Polymer tracer diffusion in multiwall carbon nanotube (MWCNT)/polymer nanocomposites is reported. As previously reported for SWCNT/polystyrene (PS) nanocomposites, the tracer diffusion of 680k deuterated polystyrene (dPS) is strongly suppressed at low MWCNT concentrations and then increases at higher concentrations. In contrast, the tracer diffusion of 10k dPS and 75k dPS is independent of MWCNT loading. These results reveal an important criterion for exhibiting a minimum in the tracer diffusion coefficient ( $D_{\min}$ ) with nanoparticle concentration, namely the relative size of tracer molecule and nanoparticle. Specifically, when the radius of gyration of the tracer polymer ( $R_g$ ) is smaller than the radius of the nanotube particle ( $R_{\text{CNT}}$ ), the tracer diffusion is independent of nanoparticle concentration, while a  $D_{\min}$  is observed when  $R_g > R_{\text{CNT}}$ . When the tracer molecule is large relative to the nanoparticle, the diffusion in the vicinity of the nanoparticle appears to become anisotropic, which leads to a  $D_{\min}$  with increasing nanoparticle loading.

## 1. Introduction

Multiwall carbon nanotubes (MWCNTs) were first identified by Sumio Iijima using high-resolution transmission electron microscopy.<sup>1</sup> MWCNTs consist of multiple concentric cylinders of carbon  $sp^2$  bonds separated by  $\sim 0.3$ – $0.4$  nm, the spacing between graphene sheets in graphite.<sup>2</sup> The diameter of the MWCNTs varies from several nanometers to tens of nanometers depending on the number of concentric nanotubes stacked into a MWCNT. The nanotube length ranges from hundreds of nanometers to a few millimeters. Compared to single wall carbon nanotubes (SWCNTs), MWCNTs are generally easier to disperse in polymer matrices as individual tubes.<sup>3</sup> As with SWCNTs, the MWCNTs exhibit remarkable electrical, thermal, and mechanical properties<sup>4–6</sup> and have been widely used to improve polymer properties by making nanocomposites.<sup>7,8</sup> MWCNTs provide nanocomposites with numerous advantages with direct applications to electronics, permeable membranes, and other materials applications.<sup>9,10</sup>

Nanocomposite properties are determined in part by the inherent properties of the nanoparticles as well as the properties of the polymer matrix. Moreover, the matrix properties in a polymer nanocomposite can differ from the bulk polymer. The properties of the polymers in the vicinity of the tube surface can be influenced by the nanoparticle or nanotubes and, thereby, differ from the bulk.<sup>11–14</sup> The nanometer size of the MWCNTs produces an extremely large quantity of interfacial area in the polymer nanocomposites, and as a result, the volume fraction of polymer near the polymer/matrix interface can be significant.<sup>5</sup> Thus, in addition to probing the properties of polymer nanocomposites that result from the combination of nanoparticle and polymers, efforts are underway to isolate the properties of the polymers in the presence of nanoparticles, including the glass transition.<sup>15</sup>

Diffusion studies are one attempt to measure a polymer-specific property in nanocomposites. Typically, diffusion shows a monotonic increase or decrease with nanoparticle concentration.<sup>16–18</sup> Merkel et al. have reported that gas and large organic molecules have an improved permeability in fumed silica/poly(4-methyl-2-pentene) nanocomposites due to the increase in the polymer free volume fraction with the addition of the nanoparticles, while in ZnO/rubber nanocomposites, the gas permeability decreases due to the increased diffusion path.<sup>19</sup> In the carbon nanotube (CNT) nanocomposites, an increase in gas permeability has been reported, but the reason for the increase is complicated. For example, rapid diffusion can result from the nanogaps surrounding the CNTs<sup>20</sup> or through the tubes and the interstitial pores between the tubes.<sup>21</sup> Therefore, other techniques are necessary to measure dynamics in carbon nanotube nanocomposites.

We recently measured polymer tracer diffusion in nanocomposites as a function of SWCNT loading to observe polymer dynamics in the presence of nanoparticles.<sup>22</sup> With increasing SWCNT concentration the tracer diffusion coefficient exhibits a minimum. The critical concentration at which the minimum in diffusion coefficient exists is comparable to the dynamic percolation threshold found in linear viscoelastic measurements. A minimum in tracer diffusion coefficient was found for four combinations of tracer and matrix molecular weight. We hypothesized that this minimum is the consequence of anisotropic diffusion near the nanotube surface, wherein polymers diffuse more slowly in the direction perpendicular to the nanoparticle surface than along the nanotubes (Figure 1). This idea was tested by simulating the center-of-mass diffusion through a three-dimensional set of cylindrical diffusion. At low trap concentrations corresponding to isolated nanotubes, the tracer diffusion decreases, while at higher trap concentrations the traps percolate and the tracer can diffuse along the interconnected traps. Here we explore the importance of the relative size of the tracer polymer and the nanoparticles. By using MWCNTs with diameters of tens of nanometers and a range of tracer polymer molecular weight, this paper studies the tracer diffusion in systems

\*Corresponding author: tel 215.898.0593; fax 215.573.2128; e-mail winey@seas.upenn.edu.

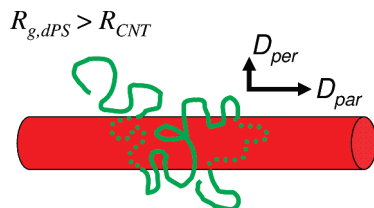


**Figure 1.** Schematic of locally anisotropic tracer diffusion in the vicinity of carbon nanotubes (red) when the radius of gyration ( $R_{g,dPS}$ ) of the tracer polymer is larger than the radius of the nanoparticles.<sup>22</sup> Near the nanotubes the diffusion coefficient in the direction of perpendicular to the nanotube surface ( $D_{per}$ ) is slower than the diffusion coefficient parallel to the nanotube ( $D_{par}$ ).

**Table 1.** Weight-Average Molecular Weight ( $M_w$ ) and Polydispersity Index (PDI) of Polystyrene (Matrix) and Deuterated Polystyrenes (Tracer), As Measured by Size Exclusion Chromatography

name	$M_w$ (kg/mol)	PDI
480k PS	478.7	1.03
10k dPS	9.6	1.04
75k dPS	76.9	1.03
680k dPS	678.4	1.10

wherein the tracer polymers are smaller than and greater than the nanotube diameters. By combining the results from SWCNT and MWCNT nanocomposites, we conclude that the tracer polymer must be larger than the nanotube to exhibit a minimum in the trace diffusion coefficient.

## 2. Experimental Section

**2.1. Materials.** Multiwall carbon nanotubes were synthesized by a chemical vapor deposition (CVD) method from Nanolab, Inc. Raw MWCNTs were purified by thermal oxidation and a HCl treatment as described in previous work.<sup>23,24</sup> The residual metal is less than 2 wt %, as measured by thermal gravimetric analysis. The MWCNTs were dispersed in *N,N*-dimethylformamide (DMF) at a concentration of 0.1 mg/mL to characterize its size. After sonicating the MWCNT/DMF suspension for 24 h, one drop of the MWCNT/DMF suspensions was removed for scanning electron microscopy (SEM). The SEM images were taken with various magnification to measure the diameter and length using a high-resolution scanning electron microscope (JEOL 4000EX). The MWCNTs were well dispersed in DMF and existed with a mean diameter of  $34 \pm 6.9$  nm, a mean length of  $871 \pm 313$  nm, and a mean aspect ratio of 26.

Polystyrenes (PS) and deuterated polystyrenes (dPS) were purchased from Pressure Chemical and Polymer Source and all used as received. Table 1 provides the molecular weights of PS and dPS by size exclusion chromatography (SEC).

**2.2. Bilayer Sample Preparation.** The bilayer sample for the diffusion study is composed of a thick nanocomposite film (matrix) and a thin dPS film (tracer). The MWCNT/480k PS nanocomposites with 0–4.7 vol % MWCNT were prepared by the coagulation method<sup>25</sup> as detailed previously for our single wall carbon nanotube/polystyrene nanocomposites.<sup>22</sup> The nanocomposite matrices were hot pressed between a silicon wafer and a piece of glass, and the thickness of the matrix layer is  $> 10 \mu\text{m}$ .

Tracer diffusion experiments require that the dPS layers be thin to minimize the dPS–dPS interactions and to avoid perturbing the polymer nanocomposite. The 75k dPS and 680k dPS films were prepared by spin-coating dPS toluene solutions on silicon substrates. Because the 10k dPS is below the entanglement molecular weight, the 10k dPS tracer was blended with 480k PS (the matrix polymer) at a weight ratio of 9/4 and co-spin-cast. The addition of 480k dPS provides mechanical integrity while transferring the tracer film onto the polymer nanocomposites. The deuterated films were floated off Si substrates onto the surface of water and then picked up with the

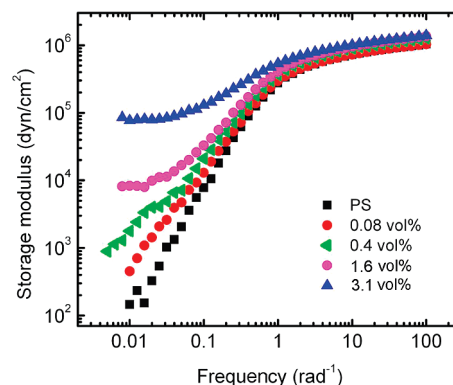


**Figure 2.** Shear storage modulus of the MWCNT/480k PS nanocomposites at various nanoparticle concentrations at 200 °C. A rheological transition from liquidlike behavior to solidlike behavior occurs at  $\sim 1.6$  vol % MWCNTs.

thick nanocomposite films. The thickness of the tracer layer is  $\sim 20$  nm, as measured by ellipsometry. The prepared bilayer film was dried for 2 days prior to annealing.

**2.3. Rheological Properties of the MWCNT Composites.** The linear viscoelastic behavior of the nanocomposites was measured on a Rheometrics Solids Analyzer II using the sandwich fixture. Samples were annealed at 200 °C for 0.5 h before testing. The modulus was measured using a frequency sweep under  $N_2$  (gas) at 200 °C with 0.5% strain.

The rheological response determines the dynamic percolation threshold of the MWCNT/PS nanocomposites.<sup>26–28</sup> Figure 2 shows the storage modulus of the nanocomposites as a function of frequency at various MWCNT concentrations. The pure polystyrene exhibits a terminal relaxation behavior with a slope of 2 at low frequencies. With increasing MWCNT concentration solidlike behavior occurs as the modulus of the nanocomposites becomes independent of frequency in the low-frequency regime, indicating the formation of a MWCNT network in the nanocomposites. The dynamic percolation threshold in these MWCNT/480k PS nanocomposites is  $\sim 1.6$  vol % MWCNT. The polymer local relaxation time is  $\sim 8$  s and is independent of MWCNT loading. At high frequency, the plateau moduli of the nanocomposites are comparable to the 480k PS homopolymer ( $G_N^0 = \sim 1.3 \times 10^5$  Pa), suggesting that the nanotubes have no significant influence on the average entanglement molecular weight of the polymer chains.

**2.3. Diffusion Measurement.** The diffusion of dPS into nanocomposites was activated by isothermally annealing the bilayer samples in custom-built vacuum ovens. These ovens have greaseless copper seals for a cleaner environment and maintain a uniform temperature to within  $< 2$  °C. The annealing temperatures were chosen based on the molecular weight of the dPS: 140 °C for 10k dPS, 150 °C for 75k dPS, and 170 °C for 680k dPS. Annealed samples were quenched to room temperature, which is below the glass transition temperature, to arrest the polymer diffusion.

Concentration profiles of dPS in the MWCNT/PS nanocomposites were measured by elastic recoil detection (ERD) and used to determine the tracer diffusion coefficient.<sup>29</sup> The ERD conditions include  $He^{2+}$  ions (3 MeV), 15° glancing angle, and a  $\sim 5 \times 5$  mm<sup>2</sup> spot size. In these experiments, the ERD sampling depth is  $\sim 800$  nm, and the depth resolution is  $\sim 80$  nm. The ERD data (counts versus energy) are converted to dPS concentration as a function of sample depth. Fick's second law gives the volume fraction profile for dPS tracer diffusion into a semi-infinite matrix as

$$\phi(x) = \frac{1}{2} \left[ \operatorname{erf} \left( \frac{h-x}{\sqrt{4Dt}} \right) + \operatorname{erf} \left( \frac{h+x}{\sqrt{4Dt}} \right) \right] \quad (1)$$

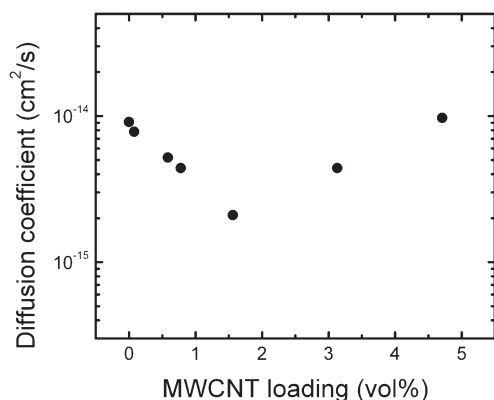


**Figure 3.** 680k dPS tracer diffusion coefficient at 170 °C in the MWCNT/480k PS nanocomposites as a function of MWCNT loading. A minimum diffusion coefficient occurs at the MWCNT concentration of 1.6 vol %.

where  $\phi(x)$  is the dPS volume fraction at depth  $x$ ,  $h$  is the thickness of the original dPS layer,  $t$  is the diffusion time,  $D$  is the tracer diffusion coefficient, and  $\text{erf}$  denotes the error function. By selecting a  $D$  and convoluting  $\phi(x)$  with the instrumental resolution, theoretical profiles from eq 1 are fit to the experimental profiles. Quality fits were obtained indicating that a single diffusion coefficient is sufficient to describe diffusion in these experiments, and our previous work demonstrates that our measured diffusion coefficients in the absence of carbon nanotubes are consistent with previously published values.<sup>22</sup>

### 3. Results

**3.1. High Molecular Weight Tracer Has a Minimum Diffusion Coefficient.** The bilayer films of 680k dPS on MWCNT/480k PS nanocomposites were thermally annealed at 170 °C. The dPS concentration profile was measured by ERD at room temperature, and the tracer diffusion coefficients ( $D$ ) were obtained by fitting the dPS depth profile.<sup>22</sup> Figure 3 shows the tracer diffusion coefficient of 680k dPS in the MWCNT/480k nanocomposites as a function of MWCNT concentration. With increasing nanoparticle loading,  $D$  decreases from  $9.1 \times 10^{-15} \text{ cm}^2/\text{s}$  for pure polystyrene to  $2.2 \times 10^{-15} \text{ cm}^2/\text{s}$  for nanocomposites with 1.6 vol % MWCNTs. The diffusion coefficient recovers as the nanotube concentration increases beyond 1.6 vol %. For example,  $D$  is  $9.6 \times 10^{-15} \text{ cm}^2/\text{s}$  at the MWCNT concentration of 4.7 vol %. A minimum in the diffusion coefficient occurs at 1.6 vol % SWCNTs, which is also the critical nanoparticle loading ( $\phi_{\text{crit}}$ ) determined rheologically. At  $\phi = \phi_{\text{crit}}$ , the normalized minimum diffusion coefficient ( $D_{\text{min}}/D_0$ ) is 0.24. Note that while  $D$  changes nonmonotonically from 0 to 4.7 vol % MWCNT, there is no substantial change in the plateau modulus (Figure 2) and thereby the average entanglement molecular weight.

The minimum in the tracer diffusion coefficient for 680k dPS in MWCNT/480k PS nanocomposites is fully consistent with our recent study of dPS tracer diffusion in SWCNT/PS nanocomposites.<sup>22</sup> In that study we hypothesized that the nanoparticles perturb the confining tubes such that the simple reptation model fails in the presence of nanoparticles. Moreover, we proposed that the diffusion is locally anisotropic such that diffusion perpendicular to the nanotube ( $D_{\text{per}}$ ) is slower than diffusion along the nanotube ( $D_{\text{par}}$ ). The ramifications of this supposition were simulated using a cylindrical trap model that defines only a spatial range over which  $D_{\text{par}} > D_{\text{per}}$  and a relative difference between  $D_{\text{per}}$  and  $D_{\text{par}}$ . At present,  $D_{\text{par}}$  is set equal to the diffusion

coefficient away from the nanotubes in the matrix. The three-dimensional simulations of the center-of-mass diffusion exhibit a  $D_{\text{min}}$  as the trap concentration increases. At low concentrations, the traps are isolated and the overall diffusion slows. With increasing concentration, the nanotubes percolate and span the polymer matrix. Thus, the diffusion traps are connected with each other, and the tracer molecules are able to diffuse within a continuous network of traps. Therefore, the diffusion coefficient recovers at high trap concentrations and produces a minimum in the diffusion coefficient. The simulations of  $D$  using the cylindrical trap model capture the  $D_{\text{min}}$  found previously for dPS tracer diffusion in SWCNT/PS nanocomposites and reported here for 680k dPS tracer diffusion in MWCNT/480k PS nanocomposites (Figure 3).

**3.2. Low Molecular Weight Tracers Have Constant Diffusion Coefficients.** To further understand the polymer tracer diffusion in the presence of carbon nanotubes, we used dPS with molecular weights of 10k and 75k g/mol as tracer polymers. In our previous diffusion studies in SWCNT/PS nanocomposites and the results presented above with MWCNT/PS nanocomposites, the tracer polymer molecules are larger than the mean radii of the nanotube particles. For example, the mean radius of the SWCNT bundles is 4.8 nm, while the shortest tracer chain we used in our previous work (75k dPS) has a size of  $R_{\text{g,dPS}} = 7.2 \text{ nm}$ .<sup>30</sup> Unlike our previous work, the tracer polymers in this section are smaller than the mean nanoparticle diameter. The tracer polymer size is described by the radius of gyration ( $R_{\text{g}}$ ):<sup>30</sup>

$$R_{\text{g}} = \frac{a\sqrt{N}}{\sqrt{6}} = \frac{a\sqrt{M_w/M_0}}{\sqrt{6}} \quad (2)$$

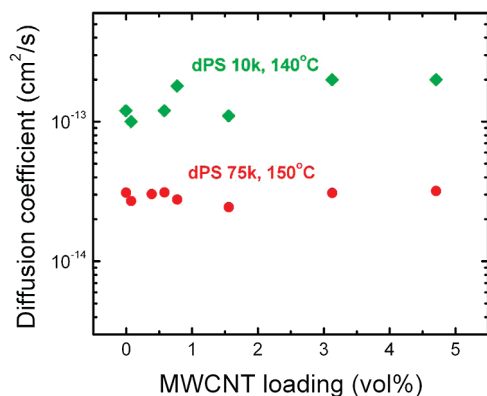
where  $M_w$  and  $M_0$  are the weight-averaged molecular weight and the molar mass of the monomeric unit, respectively, and  $a$  is the monomer length. For deuterated polystyrene,  $a = 0.67 \text{ nm}$  and  $M_0 = 112 \text{ g/mol}$ .<sup>31</sup> Thus, the size of the tracer polymers are  $R_{\text{g,dPS}}$  (10k dPS) = 2.5 nm and  $R_{\text{g,dPS}}$  (75k dPS) = 7.2 nm. In comparison, the mean radius of the MWCNTs is larger with  $R_{\text{MWCNT}} = 17 \text{ nm}$ , as measured by SEM.

Figure 4 shows the diffusion coefficients of 10k dPS and 75k dPS in the MWCNT nanocomposites as a function of nanoparticle loadings. In both cases, the diffusion coefficients are independent of MWCNT loadings. The mean tracer diffusion coefficients for 10k dPS and 75k dPS are  $(1.5 \pm 0.4) \times 10^{-13} \text{ cm}^2/\text{s}$  at 140 °C and  $(2.9 \pm 0.3) \times 10^{-14} \text{ cm}^2/\text{s}$  at 150 °C, respectively. The standard deviations for these mean diffusion coefficients are 10%–26% of the mean values. The Maxwell model for diffusion in a heterogeneous medium with impenetrable obstacles predicts<sup>32</sup>

$$\frac{D}{D_0} = \frac{1-\phi}{1+\phi/2} \quad (3)$$

where  $D$  and  $D_0$  are the diffusion coefficients with and without obstacles, respectively, and  $\phi$  is the volume fraction of obstacles. At  $\phi = 0.05$  (5 vol % nanoparticles), the Maxwell model predicts a reduction in  $D$  of  $< 8\%$  ( $D/D_0 = 0.927$ ). Within experimental error of our experiments, this small decrease in  $D$  is consistent with  $D$  being independent of nanoparticle concentration. Thus, our results do not contradict the Maxwell model for tracer diffusion of 10k dPS and 75k dPS in MWCNT/480 PS nanocomposites with up to 5 vol % nanoparticles, wherein  $D$  is essentially independent of nanoparticle concentration (Figure 4).





**Figure 4.** 10k dPS and 75k dPS tracer diffusion coefficients in the MWCNT/480k PS nanocomposites as a function of nanoparticle loadings. The diffusion occurs at 140 and 150 °C for 10k dPS and 75k dPS, respectively. The diffusion coefficients are independent of MWCNT concentration.

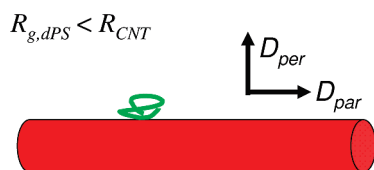


**Figure 5.** Schematic of local tracer diffusion in carbon nanotube/polymer nanocomposites, when  $R_{g,dPS} < R_{CNT}$ . Tracer diffusion near nanotubes is comparable in the directions of perpendicular and parallel to the surface ( $D_{per} \approx D_{par}$ ).

In contrast, the tracer diffusion coefficients for 680k dPS into these same nanocomposites exhibit a pronounced minimum at 1.6 vol % MWCNT (Figure 3). The distinction between these two cases is the relative size of the tracer molecule to the MWCNT radius. The higher tracer molecular weight (680k dPS) has a radius of gyration that is larger than the MWCNT:  $R_{g,dPS}$  (680k dPS) = 21.3 nm,  $R_{MWCNT}$  = 17 nm. In combination, Figures 3 and 4 identify a criterion for the tracer diffusion to exhibit a minimum as a function of MWCNT concentration. When  $R_{g,dPS} > R_{MWCNT}$ , the tracer diffusion changes nonmonotonically with increasing MWCNT concentration, as is consistent with locally anisotropic diffusion near the carbon nanotubes (Figure 1). However, when  $R_{g,dPS} < R_{MWCNT}$ , then the tracer diffusion is independent of MWCNT concentration. The absence of a minimum in the tracer diffusion coefficient is consistent with comparable local diffusion both parallel and perpendicular near the nanotube,  $D_{par} \sim D_{per}$  (Figure 5).

#### 4. Discussion

While Figures 3 and 4 compare the effect of tracer molecular weight when diffusing into the same MWCNT/480k PS nanocomposites, Figure 6 shows the influence of nanoparticle size. Both sets of data correspond to the same tracer polymer (75k dPS) and matrix polymer (480k PS). The distinction between the two sets of data is the nanoparticle type, SWCNT and MWCNT. Tracer diffusion in nanocomposites with SWCNTs exhibits a  $D_{min}$  with increasing nanotube concentration, while  $D$  is independent of nanotube concentration when the nanocomposites contain MWCNT. As above, the difference between these two cases is the relative size of the tracer polymer and the nanoparticles. The tracer polymer size ( $R_{g,75k dPS}$  = 7.2 nm) is larger than the SWCNT bundles ( $R_{SWCNT}$  = 4.8 nm) and smaller than the MWCNTs ( $R_{MWCNT}$  = 17 nm). As described above, the criterion for observing  $D_{min}$  is that the tracer polymer

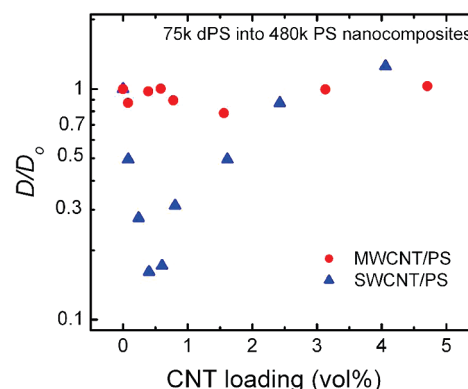


**Figure 6.** Normalized tracer diffusion coefficient ( $D/D_0$ ) of 75k dPS in MWCNT/480k PS (red) and SWCNT/480k PS (blue) nanocomposites at 150 °C.  $D/D_0$  exhibits a minimum in SWCNT nanocomposites as a function of CNT loading, while  $D/D_0$  is constant in MWCNT nanocomposites.

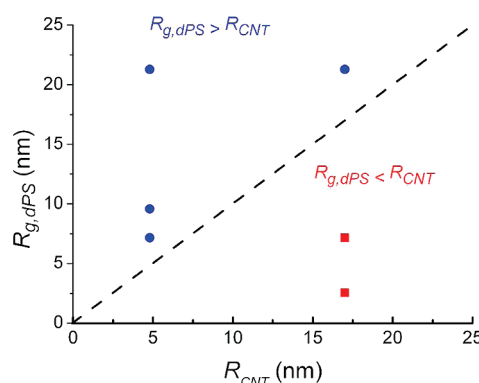


**Figure 7.** Summary of results of tracer diffusion experiments in carbon nanotube/480k PS nanocomposites including data from SWCNTs ( $R_{CNT}$  = 4.6 nm)<sup>22</sup> and MWCNTs ( $R_{CNT}$  = 17 nm) and various tracer molecular weights represented by  $R_{g,dPS}$ . Blue symbols indicate the systems that exhibit a minimum tracer diffusion coefficient with increasing nanotube concentration (see Figure 3), while red symbols correspond to systems without a minimum (see Figure 4). Dashed line represents  $R_{g,dPS} = R_{CNT}$ .

is larger than the carbon nanotube. Furthermore, when the tracer polymer is 680k dPS ( $R_{g,680k dPS}$  = 21.3 nm) (data not shown), nanocomposites with SWCNT and MWCNT both exhibit a  $D_{min}$  because in both cases  $R_{g,dPS} > R_{CNT}$ .

Figure 7 summarizes the results from tracer diffusion studies in both SWCNT and MWCNT nanocomposites by plotting the tracer polymer radius of gyration ( $R_g$ )<sup>30</sup> versus the radius of the nanotube particle ( $R_{CNT}$ ). The shape of the points indicates the presence (sphere) or absence (square) of a  $D_{min}$  with increasing nanoparticle concentration. All six systems shown in Figure 7 used a matrix of 480k PS. In addition, the system corresponding to  $R_{g,dPS}$  = 9.6 nm and  $R_{CNT}$  = 4.8 nm was also found to have a  $D_{min}$  with a 125k PS matrix.<sup>22</sup> Figure 7 reveals that for both SWCNT and MWCNT nanocomposites  $D_{min}$  was observed when the tracer polymer is larger than the width of the nanotube ( $R_{g,dPS} > R_{CNT}$ ). In contrast, the  $D_{min}$  is absent for the condition  $R_{g,dPS} < R_{CNT}$ .

At first, this finding might appear inconsistent with results we previously reported for tracer diffusion in SWCNT/480k PS nanocomposites. Figure 5c of ref 22 shows the relative tracer diffusion coefficient ( $D/D_0$ ) for three tracer polymers, and the deepest minimum corresponds to the lowest tracer molecular weight. In other words, the influence of SWCNT concentration weakens as the tracer molecular weight increases, which corresponds to larger  $R_{g,dPS}$ . Thus, one might extrapolate that a very

large tracer molecular weight could eliminate  $D_{\min}$ . Combining this earlier finding with Figure 7 indicates that the presence of  $D_{\min}$  requires an intermediate range of tracer molecular weight. The tracer polymer must be at least as large as the nanoparticle diameter, but the effect could be lost when the tracer polymer is very much larger than the nanoparticle.

We have previously associated  $D_{\min}$  with locally anisotropic diffusion in the vicinity of the nanotubes (Figure 1), and these new results further the understanding of the local dynamics by highlighting the importance of relative size. When the tracer molecules are smaller than the nanoparticles, the diffusion coefficient in nanocomposites is the same as in pure polymer, and the nanoparticles have no significant influence on tracer diffusion. This is the case shown in Figure 5, where  $D_{\text{par}} \sim D_{\text{per}}$ , because the tracer polymer is too small to be significantly entangled with the carbon nanotubes. Thus, when the nanoparticles are large with respect to the tracer polymers ( $R_{\text{CNT}} > R_{\text{g,dPS}}$ ), the excluded volume from impenetrable nanoparticles is negligible at these low loadings ( $< 5$  vol %), so that the nanotubes have no significant effect on diffusion in nanocomposites. However, when the tracer polymers are large relative to the nanoparticles ( $R_{\text{g,dPS}} > R_{\text{CNT}}$ ), the nanoparticles have a strong effect on tracer diffusion. In this regime, the presence of nanoparticles slows polymer tracer diffusion until the nanoparticle concentration reaches the percolation threshold and the tracer diffusion begins to recover. Over this same concentration regime, the plateau modulus is constant, suggesting that the average entanglement molecular weight is fixed. When  $R_{\text{g,dPS}} > R_{\text{CNT}}$ , nanoparticles appear to be capable of inducing locally anisotropic diffusion (Figure 1). The molecular mechanism associated with slower diffusion away from the nanoparticles might arise from local constraints induced by the carbon nanotubes on the confining tube of the reptation mechanism. While additional experimental and theoretical work is required to further develop the molecular mechanism, this study unambiguously reveals the importance of the relative size of the tracer molecule and the nanoparticle on the polymer tracer diffusion.

## 5. Conclusions

Polymer tracer diffusion of dPS in the MWCNT/polystyrene nanocomposites was studied for three tracer molecular weights. Combining the results from this study with earlier tracer diffusion studies in SWCNT/PS nanocomposites, we report that the tracer diffusion is independent of nanotube concentration (0–5 vol %) when the tracer polymers ( $R_{\text{g,dPS}}$ ) is small relative to the nanoparticle ( $R_{\text{CNT}}$ ). In contrast, the tracer diffusion coefficient exhibits a minimum with increasing nanotube concentration when  $R_{\text{g,dPS}} > R_{\text{CNT}}$ . This minimum is consistent with locally anisotropic diffusion near the nanotubes such that diffusion perpendicular to the nanoparticle is slower than along the nanotubes. We report that this anisotropic diffusion requires the tracer polymer to be larger than the nanotube radius. This important insight informs the ongoing effort to develop a detailed molecular mechanism of polymer dynamics in the presence of nanoparticles.

**Acknowledgment.** This research was funded by the National Science Foundation MRSEC-DMR05-20020 (K.I.W., R.J.C.) and Polymer Programs DMR05-49307 (R.J.C.). N.C. gratefully

acknowledges the award of an Overseas Travel Grant, EP/E050794/1, from the EPSRC. The authors gratefully acknowledge the use of the size exclusion chromatograph in Prof. Shu Yang's laboratory at the University of Pennsylvania. The authors thank Sadie White for valuable discussions and Dr. Chen Xu and Dr. Doug Yates for assistance with the experiments.

## References and Notes

- (1) Iijima, S. *Nature* **1991**, 354 (6348), 56–58.
- (2) Merkoci, A. *Microchim. Acta* **2006**, 152, 157–174.
- (3) Qian, D.; Dickey, E. C.; Andrews, R.; Rantell, T. *Appl. Phys. Lett.* **2000**, 76 (20), 2868–2870.
- (4) Ebbesen, T. W.; Lezec, H. J.; Hiura, H.; Bennett, J. W.; Ghaemi, H. F.; Thio, T. *Nature* **1996**, 382 (6586), 54–56.
- (5) Winey, K. I.; Vaia, R. A. *MRS Bull.* **2007**, 32 (4), 314–319.
- (6) Ruoff, R. S.; Lorents, D. C. *Carbon* **1995**, 33 (7), 925–930.
- (7) Kharchenko, S. B.; Douglas, J. F.; Obrzut, J.; Grulke, E. A.; Migler, K. B. *Nat. Mater.* **2004**, 3 (8), 564.
- (8) Hu, G.; Zhao, C.; Zhang, S.; Yang, M.; Wang, Z. *Polymer* **2006**, 47, 480.
- (9) Anand, S. V.; Mahapatra, D. R. *Nanotechnology* **2009**, 20 (1), 145707.
- (10) Hinds, B. J.; Chopra, N.; Rantell, T.; Andrews, R.; Gavalas, V.; Bachas, L. G. *Science* **2004**, 303 (5654), 62–65.
- (11) Rabin, Y. *Macromolecules* **1990**, 23 (12), 3194–3196.
- (12) Deppe, D. D.; Dhinojwala, A.; Torkelson, J. M. *Macromolecules* **1996**, 29 (11), 3898–3908.
- (13) Haggemueller, R.; Fischer, J. E.; Winey, K. I. *Macromolecules* **2006**, 39 (8), 2964–2971.
- (14) Haggemueller, R.; Guthy, C.; Lukes, J. R.; Fischer, J. E.; Winey, K. I. *Macromolecules* **2007**, 40 (7), 2417–2421.
- (15) Oh, H.; Green, P. F. *Nat. Mater.* **2009**, 8 (2), 139–143.
- (16) Hill, R. J. *Phys. Rev. Lett.* **2006**, 96 (21), 216001.
- (17) Polotskaya, G. A.; Gladchenko, S. V.; Zgonnik, V. N. *J. Appl. Polym. Sci.* **2002**, 85 (14), 2946–2951.
- (18) Zhong, J. Y.; Wen, W. Y.; Jones, A. A. *Macromolecules* **2003**, 36 (17), 6430–6432.
- (19) Merkel, T. C.; Freeman, B. D.; Spontak, R. J.; He, Z.; Pinnau, I.; Meakin, P.; Hill, A. J. *Science* **2002**, 296 (5567), 519–522.
- (20) Cong, H. L.; Zhang, J. M.; Radosz, M.; Shen, Y. Q. *J. Membr. Sci.* **2007**, 294 (1–2), 178–185.
- (21) Yu, M.; Funke, H. H.; Falconer, J. L.; Noble, R. D. *Nano Lett.* **2009**, 9 (1), 225–229.
- (22) Mu, M.; Clarke, N.; Composto, R. J.; Winey, K. I. *Macromolecules* **2009**, 42 (18), 7091–7097.
- (23) Mu, M.; Winey, K. I. *J. Phys. Chem. C* **2007**, 111 (48), 17923–17927.
- (24) Zhou, W.; Ooi, Y. H.; Russo, R.; Papanek, P.; Luzzi, D. E.; Fischer, J. E.; Bronikowski, M. J.; Willis, P. A.; Smalley, R. E. *Chem. Phys. Lett.* **2001**, 350 (1–2), 6–14.
- (25) Du, F. M.; Fischer, J. E.; Winey, K. I. *J. Polym. Sci., Part B: Polym. Phys.* **2003**, 41 (24), 3333–3338.
- (26) Du, F.; Scogna, R. C.; Zhou, W.; Brand, S.; Fisher, J. E.; Winey, K. I. *Macromolecules* **2004**, 37, 9048.
- (27) Kashiwagi, T.; Fagan, J.; Douglas, J. F.; Yamamoto, K.; Heckert, A. N.; Leigh, S. D.; Obrzut, J.; Du, F.; Lin-Gibson, S.; Mu, M. et al. *Polymer* **2007**, 48, 4855.
- (28) Hough, L. A.; Islam, M. F.; Janmey, P. A.; Yodh, A. G. *Phys. Rev. Lett.* **2004**, 93 (16), 168102.
- (29) Composto, R. J.; Walters, R. M.; Genzer, J. *Mater. Sci. Eng., R* **2002**, 38 (3–4), 107–180.
- (30) Rubinstein, M.; Colby, R. H. *Polymer Physics*; Oxford University Press: New York, 2003.
- (31) Bates, F. S.; Wignall, G. D. *Phys. Rev. Lett.* **1986**, 57, 1429–1432.
- (32) Maxwell, C. *Treatise on Electricity and Magnetism*; Oxford University Press: London, 1873; Vol. 1.